Lasing properties of a cholesteric liquid crystal containing aggregation-induced-emission material

Nan Wang,[1] Julian S. Evans,[1,*] Ju Mei,[2,3] Jianhao Zhang,[1] Iam-Choon Khoo,[4] and Sailing He[1,5]

[1]*Centre for Optical and Electromagnetic Research, Zhejiang Provincial Key Laboratory for Sensing Technologies, Zhejiang University, Hangzhou 310058, China*
[2]*MOE Key Laboratory of Macromolecular Synthesis and Functionalization, Department of Polymer Science and Engineering, Zhejiang University, Hangzhou 310027, China*
[3] *Department of Chemistry, Institute for Advanced Study, Institute of Molecular Functional Materials, and State Key Laboratory of Molecular Neuroscience, The Hong Kong University of Science & Technology, Clear Water Bay, Kowloon, Hong Kong, China*
[4]*Department of Electrical Engineering, Pennsylvania State University, University Park, PA 16802, USA*
[5]*Department of Electromagnetic Engineering, JORCEP, Royal Institute of Technology, S-100 44 Stockholm, Sweden*
[*]*julian@coer-zju.org*

Abstract: We demonstrate band edge lasing action from a cholesteric liquid crystal (CLC) containing an aggregation-induced-emission (AIE) dye as gain material. AIE materials do not suffer aggregation-caused quenching, have strong resistance to photobleaching, and can show large Stokes shift. The amplified spontaneous emission (ASE) and lasing emission of the dye-doped CLC cell have been characterized, the lasing threshold has been estimated, and its resistance to photobleaching has been measured. AIE materials with their unique properties are especially suitable for acting as gain materials in liquid crystal lasers where defect structures lower the threshold for nanoscale aggregation effects. Our studies have shown that such AIE-dye-doped CLC is capable of lasing action with unusually large Stokes shift at moderate threshold with strong resistance to photobleaching.

OCIS codes: (140.2050) Dye lasers; (160.3710) Liquid crystals.

References and links

1. H. Coles and S. Morris, "Liquid-crystal lasers," Nat. Photonics **4**(10), 676–685 (2010).
2. Y. Matsuhisa, Y. Huang, Y. Zhou, S. T. Wu, Y. Takao, A. Fujii, and M. Ozaki, "Cholesteric liquid crystal laser in a dielectric mirror cavity upon band-edge excitation," Opt. Express **15**(2), 616–622 (2007).
3. T. H. Lin, Y. J. Chen, C. H. Wu, A. Y. G. Fuh, J. H. Liu, and P. C. Yang, "Cholesteric liquid crystal laser with wide tuning capability," Appl. Phys. Lett. **86**(16), 161120 (2005).
4. S. Furumi, S. Yokoyama, A. Otomo, and S. Mashiko, "Electrical control of the structure and lasing in chiral photonic band-gap liquid crystals," Appl. Phys. Lett. **82**(1), 16–18 (2003).
5. P. G. de Gennes and J. Prost, *The Physics of Liquid Crystals* (Oxford University, 1995).
6. H. de Vries, "Rotatory power and other optical properties of certain liquid crystals," Acta Crystallogr. **4**(3), 219–226 (1951).
7. V. A. Belyakov, V. E. Dmitrienko, and V. P. Orlov, "Optics of cholesteric liquid crystals," Sov. Phys. Usp. **22**(2), 64–88 (1979).
8. V. I. Kopp, B. Fan, H. K. M. Vithana, and A. Z. Genack, "Low-threshold lasing at the edge of a photonic stop band in cholesteric liquid crystals," Opt. Lett. **23**(21), 1707–1709 (1998).
9. V. A. Belyakov, "Low threshold DFB lasing in chiral liquid crystals," Ferroelectrics **364**(1), 33–59 (2008).
10. J. Schmidtke and W. Stille, "Fluorescence of a dye-doped cholesteric liquid crystal film in the region of the stop band: theory and experiment," Eur. Phys. J. B **31**(2), 179–194 (2003).
11. J. P. Dowling, M. Scalora, M. J. Bloemer, and C. M. Bowden, "The photonic band edge laser: a new approach to gain enhancement," J. Appl. Phys. **75**(4), 1896–1899 (1994).
12. H. Shirvani-Mahdavi, E. Mohajerani, and S. T. Wu, "Circularly polarized high-efficiency cholesteric liquid crystal lasers with a tunable nematic phase retarder," Opt. Express **18**(5), 5021–5027 (2010).

#253791 Received 12 Nov 2015; revised 15 Dec 2015; accepted 16 Dec 2015; published 23 Dec 2015

13. Y. Hong, J. W. Y. Lam, and B. Z. Tang, "Aggregation-induced emission: phenomenon, mechanism and applications," Chem. Commun. (Camb.) **29**(29), 4332–4353 (2009).
14. Y. Hong, J. W. Y. Lam, and B. Z. Tang, "Aggregation-induced emission," Chem. Soc. Rev. **40**(11), 5361–5388 (2011).
15. Z. Zhao, J. W. Y. Lam, and B. Z. Tang, "Aggregation-induced emission of tetraarylethene luminogens," Curr. Org. Chem. **14**(18), 2109–2132 (2010).
16. H. C. Yeh, S. J. Yeh, and C. T. Chen, "Readily synthesised arylamino fumaronitrile for non-doped red organic light-emitting diodes," Chem. Commun. (Camb.) **20**(20), 2632–2633 (2003).
17. Y. Liu, Y. Tang, N. N. Barashkov, I. S. Irgibaeva, J. W. Y. Lam, R. Hu, D. Birimzhanova, Y. Yu, and B. Z. Tang, "Fluorescent chemosensor for detection and quantitation of carbon dioxide gas," J. Am. Chem. Soc. **132**(40), 13951–13953 (2010).
18. M. Faisal, Y. Hong, J. Liu, Y. Yu, J. W. Y. Lam, A. Qin, P. Lu, and B. Z. Tang, "Fabrication of fluorescent silica nanoparticles hybridized with AIE luminogens and exploration of their applications as nanobiosensors in intracellular imaging," Chemistry **16**(14), 4266–4272 (2010).
19. J. L. Banal, J. M. White, K. P. Ghiggino, and W. W. H. Wong, "Concentrating aggregation-induced fluorescence in planar waveguides: a proof-of-principle," Sci. Rep. **4**, 4635 (2014).
20. H. Kuball, B. Weiß, A. K. Beck, and D. Seebach, "TADDOLs with unprecedented helical twisting power in liquid crystals," Helv. Chim. Acta **80**(8), 2507–2514 (1997).
21. J. Mei, J. Wang, J. Z. Sun, H. Zhao, W. Yuan, C. Deng, S. Chen, H. H. Y. Sung, P. Lu, A. Qin, H. S. Kwok, Y. Ma, I. D. Williams, and B. Z. Tang, "Siloles symmetrically substituted on their 2, 5-positions with electron-accepting and donating moieties: facile synthesis, aggregation-enhanced emission, solvatochromism, and device application," Chem. Sci. (Camb.) **3**(2), 549–558 (2012).
22. J. Mei, J. Wang, A. Qin, H. Zhao, W. Yuan, Z. Zhao, H. H. Y. Sung, C. Deng, S. Zhang, I. D. Williams, J. Z. Sun, and B. Z. Tang, "Construction of soft porous crystal with silole derivative: strategy of framework design, multiple structural transformability and mechanofluorochromism," J. Mater. Chem. **22**(10), 4290–4298 (2012).
23. R. Ozaki, T. Shinpo, and H. Moritake, "Improvement of orientation of planar cholesteric liquid crystal by rapid thermal processing," Appl. Phys. Lett. **92**(16), 163304 (2008).
24. R. Hu, C. F. A. Gómez-Durán, J. W. Y. Lam, J. L. Belmonte-Vázquez, C. Deng, S. Chen, R. Ye, E. Peña-Cabrera, Y. Zhong, K. S. Wong, and B. Z. Tang, "Synthesis, solvatochromism, aggregation-induced emission and cell imaging of tetraphenylethene-containing BODIPY derivatives with large Stokes shifts," Chem. Commun. (Camb.) **48**(81), 10099–10101 (2012).
25. C. W. Chen, H. C. Jau, C. T. Wang, C. H. Lee, I. C. Khoo, and T. H. Lin, "Random lasing in blue phase liquid crystals," Opt. Express **20**(21), 23978–23984 (2012).
26. K. Kim, S. Hur, S. Kim, S. Jo, B. R. Lee, M. H. Song, and S. Choi, "A well-aligned simple cubic blue phase for a liquid crystal laser," J. Mater. Chem. C Mater. Opt. Electron. Devices **3**(21), 5383–5388 (2015).
27. J.-L. Zhu, S.-B. Ni, C. Ping Chen, D.-Q. Wu, X.-L. Song, C.-Y. Chen, J.-G. Lu, Y. Su, and H.-P. D. Shieh, "Chiral-induced self-assembly sphere phase liquid crystal with fast switching time," Appl. Phys. Lett. **104**(9), 091116 (2014).
28. J. Zhu, W. Li, Y. Sun, J. Lu, X. Song, C. Chen, Z. Zhang, and Y. Su, "Random laser emission in a sphere-phase liquid crystal," Appl. Phys. Lett. **106**(19), 191903 (2015).

1. Introduction

Cholesteric liquid crystal (CLC) lasers are of great interest because they adopt naturally occurring self-organizing behavior to provide the needed feedback for lasing action [1–4]. Planar CLCs have a periodic helical structure, where the local director rotates along the helical axis [5]. This periodic structure with a pitch comparable to the optical wavelength has a one-dimensional photonic band gap for circularly polarized light [6]. CLC structure thus reflects circularly polarized light which has the same handedness with the helical structure if the wavelength of the light is located within the photonic bandgap. The center wavelength λ_c of the range satisfies $\lambda_c = np$, and the wavelength range $\Delta\lambda$ satisfies $\Delta\lambda = \Delta np$, where n, p and Δn are mean refractive index, pitch and birefringence of the CLC respectively [5, 7]. If CLCs are doped with gain materials, whose emission spectrum overlaps with the photonic band gap of the CLCs, the emission will be greatly enhanced and exhibit lasing activities at the photonic band edges [8,9] due to the high densities of states [8,10] and near-zero group velocity [11] in these regions. This well-established LC laser technology has the potential to enable temperature tunable, cavity free devices that have extensive applications in medical diagnostics and laser-based display [1]. However photobleaching and defect-driven aggregation of dyes have limited the viability of these devices [12].

Commonly used gain materials in CLC laser systems are organic dyes, such as DCM and PM597 [1], which however all suffer from the so-called "concentration quenching" effects.

#253791 Received 12 Nov 2015; revised 15 Dec 2015; accepted 16 Dec 2015; published 23 Dec 2015

For ordinary organic luminophores, luminescence is often weakened or quenched at high concentrations, which is the result of the formation of aggregates [13,14]. The aggregates formed by for example π–π stacking interactions, usually decay via non-radiative pathways from excited states to ground states, leading to aggregation-caused quenching [13]. Furthermore, defect structures in liquid crystal can cause nanoscale aggregation at concentrations even below the macroscopic solubility. These "concentration quenching" effects limit the concentration of dyes used in liquid crystal lasers and fluorophores are forced to be utilized as isolated single molecules in very dilute solutions. The use of dilute solutions, however, causes many problems. One of them is that the small number of dye molecules in dilute solutions can be easily photobleached by strong pumping light [13], leading to the degradation of the laser performance with time, which is one of the basic drawbacks of dye-doped liquid crystal lasers. Another problem is that the emission of dyes with low concentration is relatively weak, which limits the output power of dye-doped liquid crystal lasers. Therefore, it is desirable to use dyes with relatively high concentration in liquid crystal laser systems to solve or at least mitigate the above problems as long as such kind of dyes don't suffer from "concentration quenching" effects. There is such a class of luminogenic materials which show a property just opposite to the "concentration quenching". These materials are non-emissive in dilute solutions but become highly luminescent when their molecules are aggregated in concentrated solutions or cast into solid films, which is known as aggregation-induced-emission (AIE) [13,14]. This class of materials which increase their luminescence when aggregated are of great interest and have already been used for organic light-emitting diode (OLED) devices [15,16], fluorescence sensors [17], bioimaging [18], luminescent solar concentrators [19] and so on. The unique property of AIE materials overcomes the "concentration quenching" drawbacks of the traditional laser dyes. However the application of AIE materials as laser dyes used in CLC lasers is never explored. In this paper, we present the results of experiments conducted on AIE-dye-doped CLC to examine the feasibility of realizing band edge lasing action. We found that unlike traditional organic dyes, tiny aggregates of the AIE dye in the CLC host are still capable of giving out strong emissions. Besides, the used AIE dye show strong resistance to photobleaching and demonstrate a large Stokes shift as well. Amplified spontaneous emission and lasing action were observed at the long wavelength edge of the photonic band gap with a threshold of around 600 μJ/mm^2.

2. Experiment

A right-handed CLC sample was made by mixing 4.84 wt% of a chiral dopant (4*S*-*trans*)-2,2-Dimethyl-α, α, α', α'-tetra(1-naphthyl)-1,3-dioxolane-4,5-dimethanol (Sigma-aldrich) with a nematic liquid crystal E7 (Jiangsu Hecheng Advanced Materials Co., Ltd). The chiral dopant's structure is shown in Fig. 1(a) and it has a helical twisting power (HTP) as high as 200 μm^{-1} in K15 [20]. The long edge of the Bragg reflection band of the dye-doped CLC sample should be within the fluorescence spectrum of the AIE material to induce lasing. The AIE dye used in the experiment was a silole derivative, 1,1-dimethyl-2,5-bis(4'-benzylidenemalononitrile)-3,4-diphenylsilole (DMTPS-DCV), whose structure is shown in Fig. 1(b) [21,22]. The synthesis of DMTPS-DCV is available in the reference 22. The fluorescence and excitation wavelength of DMTPS-DCV in pure E7 has been investigated by a fluorescence spectrophotometer (F-2500, HITACHI). 1.0 wt% of DMTPS-DCV was added into the CLC host in isotropic phase and homogeneously mixed by sonication. The dye-doped CLC sample was filled into an empty cell made up with two pieces of glass separated by 10 μm spacers. The inner surfaces of the cell glass were spin-coated with polyimide layers, which had been rubbed in two orthogonal directions for a planar aligned cell with several cholesteric pitches enclosed. In order to reduce the defect lines, the sample in the liquid crystal cell was annealed at 50^{o}C for 1 minute on a hot stage and was cooled to room temperature in 2 minutes by exposing it to the air [23]. 20 cycles of the process was repeated

#253791 Received 12 Nov 2015; revised 15 Dec 2015; accepted 16 Dec 2015; published 23 Dec 2015

until the defect lines were significantly reduced. The dye-doped CLC cell was then investigated with polarizing optical microscopy (POM) and fluorescence microscopy on a Zeiss microscope (Axio Imager. M2m). The transmission and reflection spectra of the dye-doped CLC cell were also measured with a spectrometer (USB-2000, Ocean Optics) mounted on the same microscope.

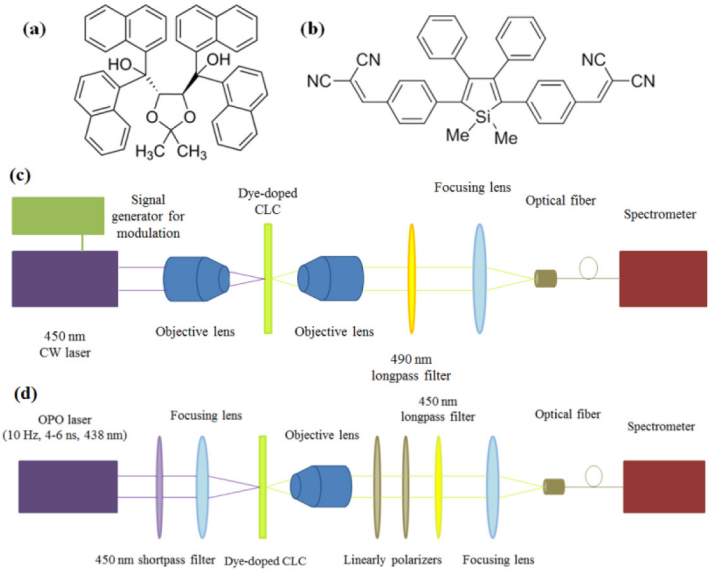

Fig. 1. (a) Chemical structure of the chiral dopant. (b) Chemical structure of the AIE material DMTPS-DCV. (c) Experimental setup for characterizing the ASE from the dye-doped CLC cell. (d) Experimental setup for inducing and characterizing the lasing emission from the dye-doped CLC cell.

Figure 1(c) demonstrates the experimental setup for measuring the amplified spontaneous emission (ASE) from the dye-doped CLC cell. The pumping laser for the dye-doped CLC cell was a continuous wave (CW) laser (MDL-III-450, Opto Engine LLC) with a wavelength of 450 nm. In order to reduce the heating effects, the CW laser was modulated by a signal generator to give out pulses, whose repetition rate was 3 kHz and the duration was ~56 μs. The pumping laser beam travelling through the focusing objective lens (20 × , NA = 0.40) can form a spot as small as 10-20 μm in diameter. However, the dye-doped CLC sample was set a little bit off focus to reduce the heating effects. The emission of the sample was collected by a 5 × objective lens (NA = 0.13) and was then focused by a convex lens with a focal length of f = 30 mm onto a multi-mode optical fiber which was connected to a spectrometer (USB-2000, Ocean Optics) before passing through a 490 nm long-pass filter. Figure 1(d) sketches the experimental setup used to characterize the lasing emission of the dye-doped CLC sample. The pumping source for the dye-doped CLC cell was a tunable Nd:YAG-Laser system NT342A (EKSPLA) which is comprised of a Q-switched Nd:YAG pumping laser, harmonics generators and optical parametric oscillator (OPO). The OPO laser which was adopted to induce the lasing emission from the dye-doped CLC cell has a tuning range from 410 nm to 2600 nm, with 438 nm as the chosen pumping wavelength. The duration of the pulse is 4-6 ns, and the repetition rate is 10 Hz, and tunable delay time allows for control of the power of the OPO laser over a large range. After passing through a 450 nm short-pass filter which was used to eliminate the residual pulse (1064 nm) and the second harmonic wave (532 nm) of the Nd:YAG laser, the pumping laser beam was focused onto the sample at a normal incidence angle forming a spot of 130 μm in diameter by a convex lens with a focal length f = 30 mm. The emission originating from the sample was collected by a 10 × objective lens (NA = 0.25)

#253791 Received 12 Nov 2015; revised 15 Dec 2015; accepted 16 Dec 2015; published 23 Dec 2015

and then focused by a convex lens with a focal length of f = 30 mm onto a multi-mode optical fiber which was connected to a spectrometer (PG2000-Pro, Ideaoptics; resolution ~0.34 nm). Two linear polarizers and a 450 nm long-pass filter between the two lenses were used to attenuate and accommodate the pumping laser and the lasing emission from the sample to the detection range of the spectrometer.

3. Results and discussions

The fluorescence spectrum of DMTPS-DCV in pure E7 with the excitation wavelength of 440 nm is shown in Fig. 2(a) demonstrating that the material's fluorescence ranges from 530 nm to 600 nm and peaks at 550 nm. The fluorescence intensity of DMTPS-DCV in E7 with the emission wavelength of 550 nm as a function of excitation wavelength depicted in Fig. 2(b) demonstrates that the most efficient wavelength for exciting DMTPS-DCV in E7 is 340nm while the wavelengths between 430 nm and 465 nm are also efficient to induce its emission. Since the tunable output wavelength of the pumping laser starts from 410 nm, we chose 438 nm as the pumping wavelength to induce laser emission from the dye-doped CLC. Compared with other conventional laser dyes, AIE materials show a large Stokes shift, due to the presence of the aromatic propeller groups [24].

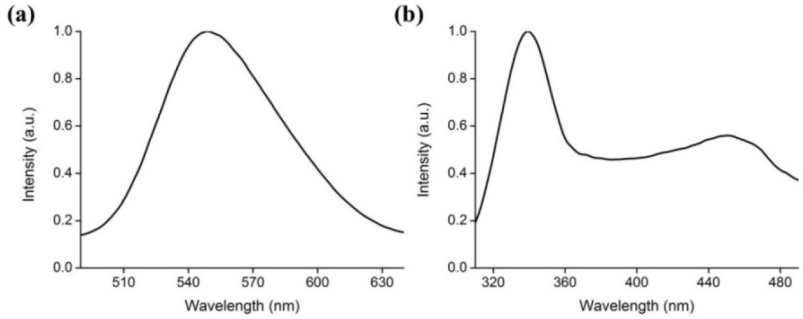

Fig. 2. (a) The fluorescence spectrum of DMTPS-DCV in E7 with the excitation wavelength of 440 nm and (b) the 550-nm fluorescence intensity of DMTPS-DCV in E7 as a function of excitation wavelength.

The POM and fluorescence microscopy image of the dye-doped CLC cell are shown in Fig. 3(a), and (b) respectively. In order to avoid scattering loss, relatively low defect line density is achieved by a small cell gap (~10 μm) and 20 cycles of annealing and cooling. The final dye-doped CLC cell mainly comprises large domains (several 100's μm by several 100's μm) of cholesteric planar structure as shown in Fig. 3(a). The uniform orange fluorescence of the dye-doped CLC sample illuminated by a UV lamp with a wavelength of 365 nm revealed in Fig. 3(b) demonstrates that AIE dyes are well dissolved in the large domains of cholesteric planar structure. Moreover, there are still some defects (such as circled area A) caused by the imperfection of rubbing and tiny crystallites (such as circled area B) of the AIE material. Both area A and B show stronger fluorescence compared with cholesteric planar domains in Fig. 3(b), which implies that the AIE material tends to aggregate in the defect and AIE aggregates are still active to give out fluorescent emissions. In an AIE-dye-doped CLC cell where liquid crystals are not well aligned and full of defects, aggregates of dyes in the defects are even more prominent and highly emissive (shown in Fig. 3(c)). Compared with traditional dyes which experience aggregation-caused quenching, tiny aggregates of the AIE dye are still capable of giving out strong emissions, thus changing the limitations associated with the low solubility of dyes or liquid crystals containing small amount of defects into advantages. The measured transmission and reflection spectra of the dye-doped CLC cell are shown in Fig. 3(d). Adding AIE dye to CLC host will affect the position of the CLC reflection band mainly in the form of a red shift of ~17 nm. Also note that compared with undoped CLC, the

#253791 Received 12 Nov 2015; revised 15 Dec 2015; accepted 16 Dec 2015; published 23 Dec 2015

absorption by the AIE dye at the short wavelength edge region accounts for the depressed transmittance of the AIE-dye-doped CLC. Besides the reflection spectrum of the dye-doped CLC cell was measured with an aluminum mirror (reflectance ~90%) as reference, which causes the measured reflectance is over 50%.

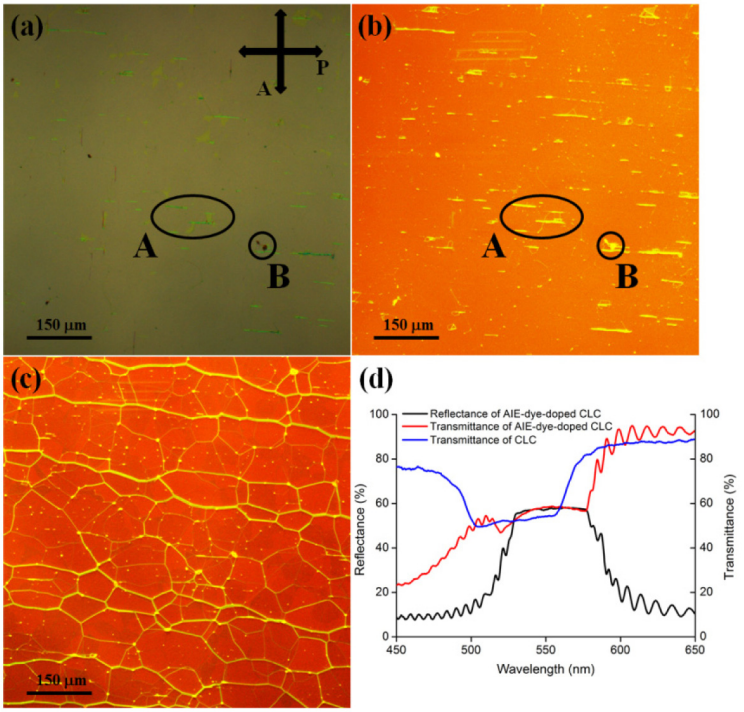

Fig. 3. (a) POM image (P and A indicate the polarization of the polarizer and the analyzer.) and (b) fluorescence microscopy image with excitation wavelength of 365 nm of the well-aligned dye-doped CLC cell. (c) Fluorescence microscopy image of the non-annealed dye-doped CLC shows significant fluorescence in the defect lines indicating dye aggregation. (d) Reflection (black line) and transmission (red line) spectra of the well-aligned AIE-dye-doped CLC cell, along with transmission spectrum (blue line) of the undoped CLC.

Figure 4(a) demonstrates the ASE spectrum of the dye-doped CLC cell induced by a modulated CW 450-nm laser. The CW power of the laser was ~0.4 W without modulation, and then the continuous wave of the laser was chopped into pulses with a repetition rate of 3 kHz and a duration time of ~56 μs by the modulation signals. The spectrum reveals ASE on the both edges of the CLC photonic band gap; note that the ASE on the long wavelength edge is much stronger than that on the short wavelength edge and it has several side modes, which indicates the AIE dye is well aligned in parallel with the local director of the CLC host [10]. Since the mode closest to the long wavelength edge (corresponding to the wavelength of 586.2 nm) has the lowest threshold, it is the easiest one to turn into a laser. Continuously increasing the power of the pumping CW laser will liquefy the CLC and destroy the planar structure.

#253791 Received 12 Nov 2015; revised 15 Dec 2015; accepted 16 Dec 2015; published 23 Dec 2015

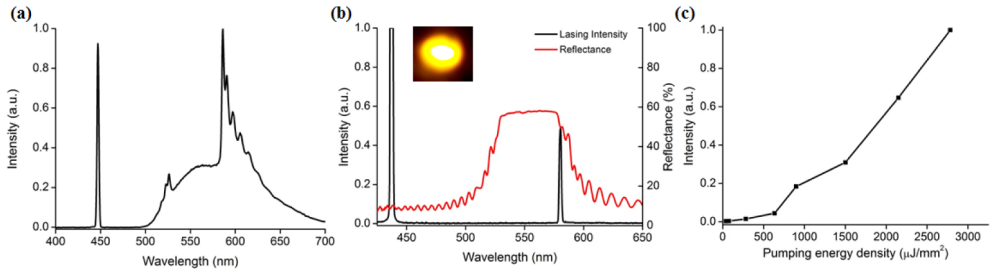

Fig. 4. (a) The ASE spectrum of the dye-doped CLC cell induced by a modulated CW laser at the pumping power lower than 0.4 W (before modulated) and with pumping wavelength of 450 nm. (b) The reflection spectrum of the dye-doped CLC cell (red line) and the lasing spectrum (black line) of the dye-doped CLC cell induced by a nanosecond pulsed laser at the pumping power of ~800 μJ/mm^2 with the pumping wavelength of 438 nm. Inset shows the far field image of the emission beam. (c) The relationship between emission output power of the dye-doped CLC cell and the pumping energy density.

Figure 4(b) demonstrates the reflection spectrum of the dye-doped CLC cell and the lasing emission spectrum of the cell induced by the nanosecond pulsed 438-nm laser at a pumping power of ~800 μJ/mm^2. It is seen that the lasing takes place at the wavelength of 580.4 nm, which is located at the long wavelength edge of the reflection band gap. The full width of half maximum (FWHM) of the lasing spectrum was measured to be 2.1 nm. The inset of Fig. 4(b) shows the far field image of the well-formed emission beam. It is seen that the AIE dye-doped CLC laser exhibits a Stokes shift of ~150 nm (250 nm is achievable with proper pumping wavelength), which is hard to be achieved with some commonly used laser dyes in liquid crystal such as DCM. Figure 4(c) shows the relationship between emission output power of the dye-doped CLC cell and the pumping energy. It is estimated that the threshold of the dye-doped CLC laser is 8.0 μJ. Considering the spot size of the pumping laser on the CLC cell was 130 μm in diameter, the pumping energy density threshold is about 600 μJ/mm^2. Besides, the CLC will be heated to isotropic phase as the pumping energy density increases.

#253791 Received 12 Nov 2015; revised 15 Dec 2015; accepted 16 Dec 2015; published 23 Dec 2015

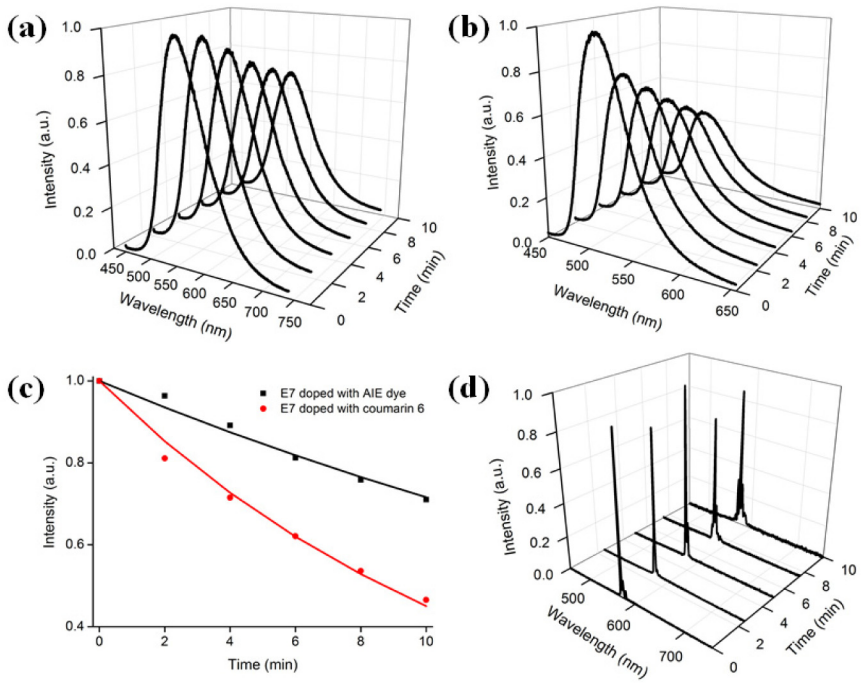

Fig. 5. (a) Time-dependent fluorescence spectra of E7 doped with 1 wt% of the AIE dye. (b) Time-dependent fluorescence spectra of E7 doped with 1 wt% of coumarin 6. (c) Time-dependent integrated fluorescence intensity of E7 doped with the AIE dye and E7 doped with coumarin 6. (d) Time-dependent lasing emission spectra of the AIE-dye-doped CLC.

Finally, the photobleaching resistance of the AIE-dye-doped CLC was explored and the AIE dye was compared with coumarin 6 (Sigma-aldrich) concerning that aspect. Coumarin 6 was chosen since it can be excited efficiently by the same 450-nm laser as the AIE material. Figure 5(a) demonstrates the time-dependent fluorescence spectra of E7 doped with 1 wt% of the AIE dye in a 20 μm thick liquid crystal cell pumped by a CW 450-nm laser with a power of ~1 W (focusing area was ~0.3 cm^2). Figure 5(b) demonstrates the time-dependent fluorescence spectra of E7 doped with 1 wt% of coumarin 6 under the same conditions. It is seen that the fluorescence intensity of both samples dropped due to photobleaching while they were excited continuously by the high power laser, but the fluorescence intensity of the sample with coumarin 6 decreased at a much higher rate than that of the sample with the AIE dye. The time-dependent integrated fluorescence intensity of both samples in Fig. 5(c) demonstrates that AIE dye shows stronger photobleaching resistance than coumarin 6 with the same weight concentration. In addition, the viability of adopting higher concentration of AIE materials may enhance the photobleaching resistance of AIE-dye-doped CLC even further. Figure 5(d) shows the time-dependent lasing emission spectra of the AIE-dye-doped CLC pumped continuously by the aforementioned nanosecond pulsed laser with a power of ~800 μJ/mm^2. It is seen that the sample showed reasonably strong photobleaching resistance and didn't show an obvious degradation of performance (the fluctuation of the emission intensity is associated with a combination of photobleaching and the instability of the pumping power).

4. Conclusions

In this work, we have demonstrated the feasibility of a band edge CLC laser with an AIE dye as its gain material. Our preliminary studies have shown that such AIE dye-doped CLC is capable of lasing action with unusually large Stokes shift at moderate threshold (600

#253791 Received 12 Nov 2015; revised 15 Dec 2015; accepted 16 Dec 2015; published 23 Dec 2015

μJ/mm^2). This threshold can be further reduced with optimization in AIE dye concentration, sample thickness, input optics, and selection of other AIE materials. Furthermore, the sample is highly photo-stable; repeated exposure to focused high intensity laser pulse (800 μJ/mm^2 nanosecond pulses) excitation does not cause obvious degradation of performance. We have also demonstrated that tiny aggregates of the AIE dye were still capable of giving out strong emissions, thus changing the limitations associated with low solubility of dyes or liquid crystals containing small amount of defects into advantages. AIE dyes are promising gain media for a variety of laser hosts that possess topological defects such as blue phase [25,26] and "sphere phase" liquid crystals [27,28].

Acknowledgments

We thank the help from Jun Qian, Qingkun Liu and Tingbiao Guo during the experiment. This research was supported by the National Natural Science Foundation of China (Nos. 91233208 and 61178062) and the Program of Zhejiang Leading Team of Science and Technology Innovation, Swedish VR grant (# 621-2011-4620) and AOARD. Professor I. C. Khoo acknowledges the support from Sir Pao Yu-Kong Chair Professorship during his visit to Zhejiang University.

#253791 Received 12 Nov 2015; revised 15 Dec 2015; accepted 16 Dec 2015; published 23 Dec 2015